Metallic surface electronic state in half-Heusler compounds RPtBi (R= Lu, Dy, Gd)

Chang Liu, Yongbin Lee, Takeshi Kondo, Eun Deok Mun, Malinda Caudle, B. N. Harmon, Sergey L. Bud'ko, Paul C. Canfield, and Adam Kaminski

Metallic surface electronic state in half-Heusler compounds RPtBi (R = Lu, Dy, Gd)

Chang Liu[*,1,2] Yongbin Lee[*,1] Takeshi Kondo,[1,2] Eun Deok Mun,[1,2] Malinda Caudle,[1,2]
B. N. Harmon,[1,2] Sergey L. Bud'ko,[1,2] Paul C. Canfield,[1,2] and Adam Kaminski[1,2]

[1]*Division of Materials Science and Engineering, Ames Laboratory, Ames, Iowa 50011, USA*
[2]*Department of Physics and Astronomy, Iowa State University, Ames, Iowa 50011, USA*
(Dated: April 6, 2011)

Rare-earth platinum bismuth (RPtBi) has been recently proposed to be a potential topological insulator. In this paper we present measurements of the metallic surface electronic structure in three members of this family, using angle resolved photoemission spectroscopy (ARPES). Our data shows clear spin-orbit splitting of the surface bands and the Kramers' degeneracy of spins at the $\bar{\Gamma}$ and $\bar{M}$ points, which is nicely reproduced with our full-potential linearized augmented plane wave calculation for a surface electronic state. Topologically non-trivial behavior is signified by band inversion in the calculated bulk electronic structures, yet no direct indication of such behavior is detected by ARPES, except for a weak Fermi crossing detected in close vicinity to the $\bar{\Gamma}$ point, making the total number of Fermi crossings odd. In the surface band calculation, however, this crossing is explained by a Kramers' pair of bands that are very close to each other. The classification of this family of materials as topological insulators remains an open question.

PACS numbers:

I. INTRODUCTION

The discovery of topologically non-trivial states of matter opens up a new realm of knowledge for fundamental condensed matter physics. Unlike conventional materials, these "topological insulators" exhibit metallic surface states that are protected by time reversal symmetry, while maintaining an insulating bulk electronic structure. This leads to a variety of novel properties including odd number of surface Dirac fermions, strict prohibition of back-scattering, etc., paving the way to potential technical breakthroughs in e.g. quantum computing process via the application of spintronics[1,2]. Recently, extensive theoretical and experimental efforts have led to the realization of such fascinating behaviors in e.g. the HgTe quantum wells[3–5], the $Bi_{1-x}Sb_x$ system[6–8] and the Bi_2X_3 (X = Te, Se) binary compounds[9,10]. Numerous half-Heusler ternary compounds have been proposed, theoretically, to be potential new platforms for topological quantum phenomena[11,12], where the inherent flexibility of crystallographic, electronic and superconducting parameters provide a multidimensional basis for both scientific and technical exploration. The experimental determination of their topological class would set the basis for possible spintronic utilization and further studies on the interplay between the topological quantum phenomena versus e.g. the magnetic[13], superconducting[14] and heavy Fermionic[15] behaviors.

Theoretically, the topological insulators experience a gapless surface state protected by time reversal symmetry and thus are robust against scattering from local impurities. Such a surface state is "one half" of a normal metal in that the surface bands are strongly spin-polarized, forming a unique spin helical texture[7,16]. On the other hand, the Kramers' theorem requires that the spin be degenerate at the Kramers' points - k-points of the surface Brillouin zone where time reversal symmetry is preserved[17]. At the interface between, say, a normal spin-orbit system and vacuum, the spin-polarized surface bands connect pairwise (Kramers' pair), crossing the chemical potential μ an even number of times between two distinct Kramers' points. At the interface between a topologically non-trivial material and vacuum, however, one expects the surface bands to cross μ an odd number of times[1].

In this paper we present a systematic survey on the surface electronic structure of half-Heusler compounds RPtBi (R = Lu, Dy, Gd) using angle resolved photoemission spectroscopy (ARPES). Our results show clear spin-orbit splitting of the surface bands that cross the chemical potential, which is nicely reproduced in the full-potential augmented plane wave calculation for a surface electronic state. The Kramers' degeneracy of spin is unambiguously detected at both the $\bar{\Gamma}$ and $\bar{M}$ points. Although our bulk band calculation yields a band inversion typical for topologically non-trivial materials, no direct indication of such behavior is detected by ARPES, except for the fact that there is a weak Fermi crossing in the close vicinity to the $\bar{\Gamma}$ point, making a total of five crossings in the $\bar{\Gamma}$-$\bar{M}$ line segments. In the surface band calculation, however, this inner crossing is explained by two spin-orbit splitting bands that are very close to each other, forming another Kramers' pair. In this band configuration, the total Berry phase would be zero for the half-Heusler systems, and they would not be topologically non-trivial. The detailed topological class of this family of materials thus remains an open question, requiring a detailed spin-resolved ARPES study with ultra-high momentum resolution and a direct calculation of the topological invariants based on the first principle band structure.
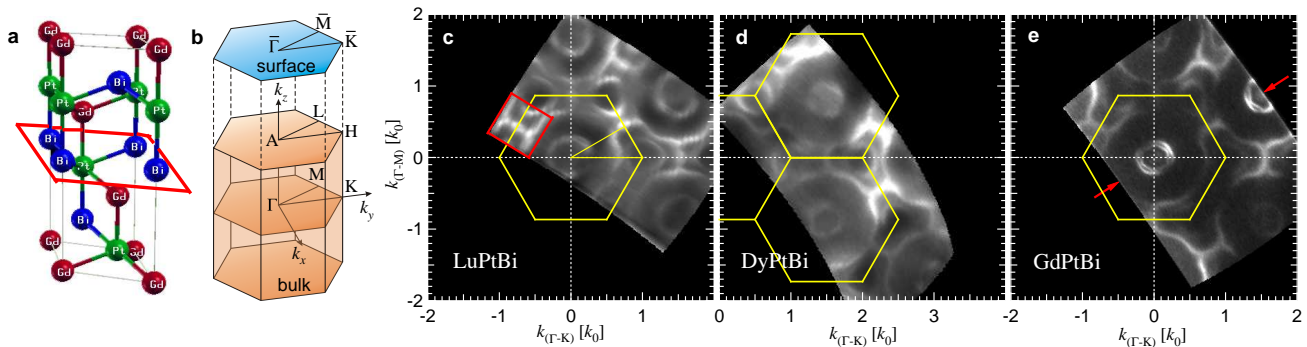
FIG. 1: (Color online) Surface Fermi maps of half-Heusler compounds RPtBi (R = Lu, Dy, Gd). (a) $C1_b$ Crystal structure of RPtBi. The crystallographic axes are rotated so that the (111) direction points along z. The red parallelogram marks the Bi(111) cleaving plane. (b) The surface and bulk Brillouin zone for the rotated crystal structure in (a). Here k_z corresponds to the (111) direction of the fcc Brillouin zone. (c)-(e) Surface Fermi maps of RPtBi. All data is taken with 48 eV photons at $T = 15$ K. Yellow lines denote the surface Brillouin zone.

II. METHODS

Single crystals of RPtBi (R = Lu, Dy, Gd) were grown out of a Bi flux and characterized by room temperature power X-ray diffraction measurements[13,18]. The crystals grow as partial octahedra with the (111) facets exposed. Typical dimensions of a single crystal are about $0.5 \times 0.5 \times 0.5$ mm^3. The ARPES measurements were performed at beamline 10.0.1 of the Advanced Light Source (ALS), Berkeley, California using a Scienta R4000 electron analyzer. Vacuum conditions were better than 3×10^{-11} torr. All ARPES data was taken at $T = 15$ K, above the magnetic ordering temperatures of all compounds[13]. The energy resolution was set at ~ 15 meV. All samples were cleaved *in situ*, yielding clean (111) surfaces in which atoms arrange in a hexagonal lattice. High symmetry points for the surface Brillouin zone are defined as $\bar{\Gamma}(0,0)$, $\bar{K}(k_0,0)$ and $\bar{M}(0, k_0\sqrt{3}/2)$ with unit momentum $k_0 = \sqrt{6}\pi/a$, where a is the lattice constant for each type of crystals. We emphasize here that no stress or pulling force is felt by the samples, which ensures that the measured data reveals the intrinsic electronic structure of the single crystals.

In the band structure and Fermi surface calculation for both the bulk and the surface, we have used a full-potential linearized augmented plane wave (FPLAPW) method[19] with local density functional[20]. The scalar relativistic method was employed and spin-orbit coupling was included by a second-variational procedure. The structural data were taken from a reported experimental result[21]. For the bulk band calculation of *cubic* GdPtBi, we used 1240 k-points in the irreducible *fcc* Brillouin zone and set $R_{MT} \times k_{max} = 9.0$, where R_{MT} is the smallest muffin-tin radius and k_{max} is the plane-wave cutoff. For the surface band calculation, since we are interested in the (111) surface we generated a hexagonal cell which has the z-axis pointing along the [111] direction of the cubic cell. After that, we constructed supercells with 3

layers and 21.87 a.u. vacuum and used these supercells to calculate the band structures. Although we calculated band structures of all 6 possible surface endings (Gd-Bi-Pt-bulk, Gd-Pt-Bi-bulk, Bi-Gd-Pt-bulk, Bi-Pt-Gd-bulk, Pt-Gd-Bi-bulk, Pt-Bi-Gd-bulk), in this paper we present just the Bi-Pt-Gd-bulk results which show good agreement with experiment [Fig. 2(b), (d)-(f)]. To obtain the self-consistent charge density, we chose 48 k-points in the irreducible Brillouin zone, and set $R_{MT} \times k_{max}$ to 7.5. We used muffin-tin radii of 2.5, 2.4 and 2.4 a.u. for Gd, Bi, and Pt respectively. For the non-magnetic calculation, the seven $4f$ electrons of Gd atoms were treated as core electrons with no net spin polarization. The atoms near the surface (Bi, Pt, Gd) were relaxed along the z-direction until the forces exerted on the atoms were less than 2.0 mRy/a.u.. As an example, in the Bi-Pt-Gd-bulk structure, the surface Bi, Pt, Gd atoms' z internal coordinates were relaxed to 0.1199, 0.1024 and 0.0829 from 0.1250, 0.1042 and 0.0833 respectively. With this optimized structure, we obtained self-consistency with 0.01 mRy/cell (1 Ry $\simeq 2.18 \times 10^{-18}$ J $= 13.62$ eV) total energy convergence. After that, we calculated the band structure and two dimensional Fermi surface ($k_z = 0.0$) in which we divided the rectangular cell connecting four $\bar{K}$-points by 40×40, yielding 1681 k-points.

III. RESULTS AND DISCUSSION

We begin this survey in Fig. 1 by showing the Fermi maps of the three half-Heusler compounds RPtBi (R = Lu, Dy, Gd). Previous theoretical calculations for the bulk electronic structure[11,12,22] suggested that the Kramers' crossing at the $\bar{\Gamma}$ point happens very close to μ; a detailed theoretical study on the band structures showed that the RPtBi series are ungapped semimetals[23]. The data in Fig. 1 shows that, in the (111) cleaving plane, there are several bands crossing μ in the vicinity
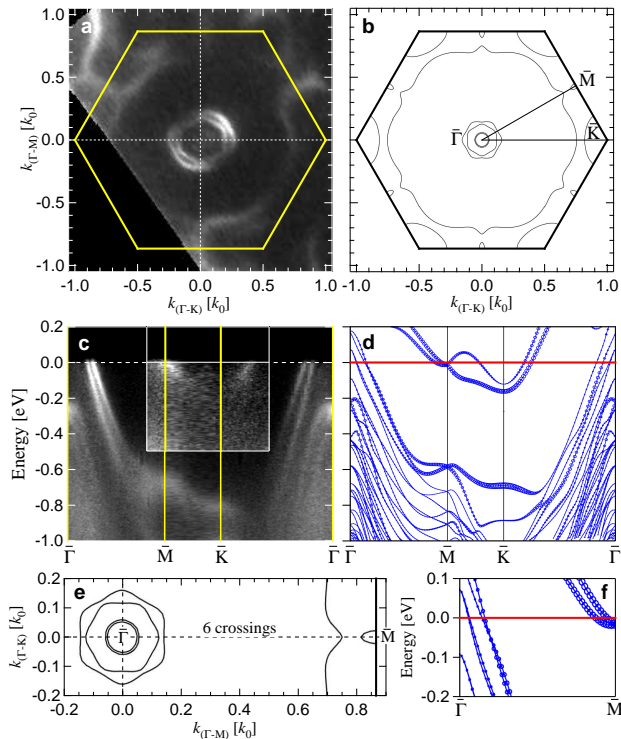
FIG. 2: (Color online) Surface electronic structure of GdPtBi: Comparison between ARPES data and calculational result. (a) Fermi map of GdPtBi observed by ARPES, same as Fig. 1(e). (b) Calculational surface Fermi map of GdPtBi at the Bi(111) cleaving plane. See text for details. (c) ARPES band structure along the contour $\bar{\Gamma}$-$\bar{M}$-$\bar{K}$-$\bar{\Gamma}$. Inset of (c) enhanced the ARPES intensity near $\bar{M}$ and $\bar{K}$ for better visibility of the bands. (d) Calculational band structure with respect to (c). Sizes of hollow circles represent the contribution of surface Pt atoms. (e)-(f) Expanded figures for (b) and (d), respectively, showing six Fermi crossings. Panel (e) is rotated by 30° with respect to (b).

of the half-Heuslers, two immediate questions follow the observations in Fig. 1: (1) Are the observed bands actually arising due to the sample surface? (2) Exactly how many times do the bands intersect the chemical potential along the $\bar{\Gamma}$-$\bar{M}$ line segment?

Fig. 2 shows the comparison between the ARPES data and a calculational surface state in GdPtBi. Even at first glance, Fig. 2 gives the impression of remarkable agreement between theory and experiment. All basic features observed by ARPES - the overall shape and location of the Fermi pockets [Fig. 2(a)-(b)], the binding energies of the bands [Fig. 2(c)-(d) - are well reproduced by the calculation. The main point of this figure, however, is the fact that band calculations show a total of six Fermi crossings along the $\bar{\Gamma}$-$\bar{M}$ line segment, which is an even number and is not directly consistent with the proposed strong topological insulating phenomenon[11,12]. In fact traces for the inner two crossings is also found in the ARPES data, where they appear to be one single crossing, most likely due to finite momentum resolution [Leftmost part in Fig. 2(c), see also Fig. 3(d)-(h)]. It should be noted that, in order to take into account the spin-orbit splitting, relativistic effects are applied to the calculation. In addition to the surface bands we also performed the same calculation for the bulk electronic structure of GdPtBi in which the band inversions at the Γ-point have been discussed as a criteria for the topological insulator[11,12]. In Ref.[25], Xiao *et al.* showed that the fourfold degenerate Γ_8 states lie above the twofold degenerate Γ_7 and Γ_6 states, as is the case for HgTe. Our bulk calculation for GdPtBi [see Fig. 3(c), details not shown] showed that while three bands were crossing the Fermi energy near the Γ-point, the band order of Γ_8, Γ_7 and Γ_6 was same as the LaPtBi bands in Ref.[25]. Similar calculations also reproduce clear topological insulating behavior in Bi_2Te_3 thin films[26]. The excellent agreement shown in Fig. 2 also implies the validity of such calculation for the surface electronic structures of the half-Heusler compounds.

In Fig. 3 we prove that the observed bands come from the sample surface. This is done by scanning the incident photon energy along both $\bar{\Gamma}$-$\bar{K}$ and $\bar{\Gamma}$-$\bar{M}$ high symmetry directions. Varying the photon energy in ARPES effectively changes the momentum offset along the direction perpendicular to the sample surface. In our case, this direction corresponds to k_z or the (111) direction of the *fcc* Brillouin zone. Figs. 3(a)-(b) show that all resolved bands form straight lines along the k_z direction, a clear indication for the lack of k_z dependence. In Fig. 3(c) we compare this to a calculated Fermi surface map for the *bulk* bands, along the same direction as in Fig. 3(a). The difference is clear: the bulk bands are dispersive along the Γ-A direction; and most of the experimentally observed bands are not present in the calculation. In Figs. 3(d)-(h) we pay special attention to the bands crossing μ near $\bar{\Gamma}$ by showing the band structure for four different photon energies. In total there are at least three Fermi contours surrounding $\bar{\Gamma}$, the outer two being a lot brighter than the
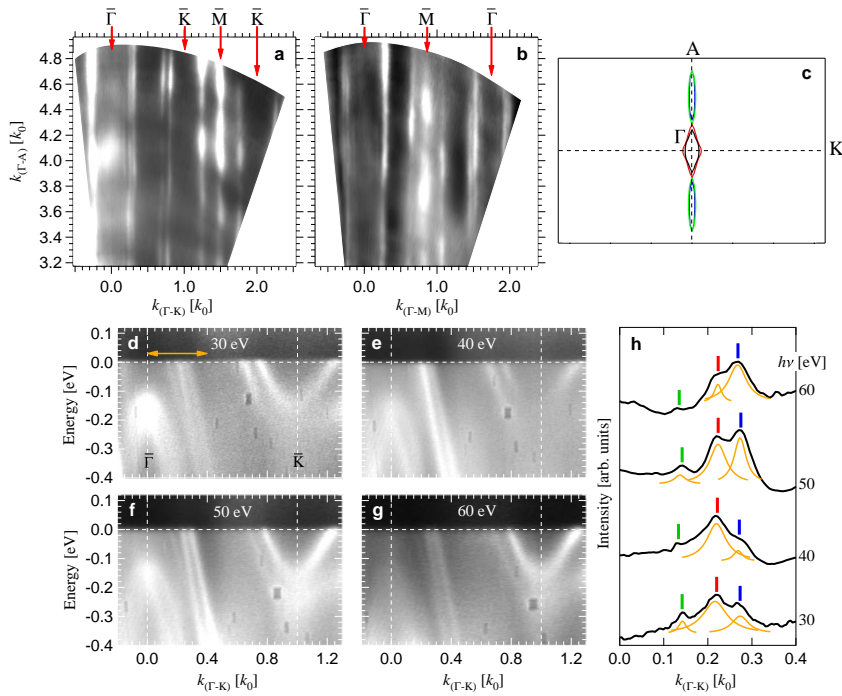
of both the $\bar{\Gamma}$ and $\bar{M}$ points. The overall Fermi surface for all three half-Heusler compounds are similar, indicating cleaving planes with the same elemental nature, and similar band structure for all members. By comparing the band structure measured at the (111) surface with results of band calculations for GdPtBi (Fig. 2), we find the cleaving plane to be Bi(111), marked by a red parallelogram in Fig. 1(a). A closer look at Fig. 1(c)-(e) reveals that the $\bar{\Gamma}$ pockets have different sizes for different half-Heusler members. For example the circular $\bar{\Gamma}$ pockets in LuPtBi are larger in size than those in GdPtBi. This indicates a different effective electron occupancy for different members of the half-Heusler family. One should also note that in Fig. 1(e) the inner of the two bright $\bar{\Gamma}$ pockets is hexagonal in shape, reminiscent of the hexagonal shape of the Dirac cone in Bi_2Te_3 (Ref.[10]), which is explained by higher order terms in the $k{\cdot}p$ Hamiltonian[24]. This hexagonal shape is very nicely reproduced in the calculation [Fig. 2(b)]. For clarifying the topological class

FIG. 3: (Color online) Absence of k_z dispersion as proof for the observation of a surface electronic structure. (a)-(b) k_z (Γ-A) dispersion maps for LuPtBi. Data is obtained by scanning the incident photon energy $h\nu$ from 30 to 80 eV along (a), the $\bar{\Gamma}$-$\bar{K}$ and (b) the $\bar{\Gamma}$-$\bar{M}$ direction. (c) Calculational Fermi surface map for the *bulk* state in the A-Γ-K plane. See panel (a) for comparison. (d)-(g) Band dispersion maps along the the $\bar{\Gamma}$-$\bar{K}$ direction for selected $h\nu$s. It is clear that all observed bands are independent of $h\nu$ (k_z). (h) Detailed peak analysis for the momentum distribution curves (MDCs) at the chemical potential for four different photon energies. k range is indicated by an orange double arrow in (d). Bars in different colors indicate the Fermi crossings for different bands.
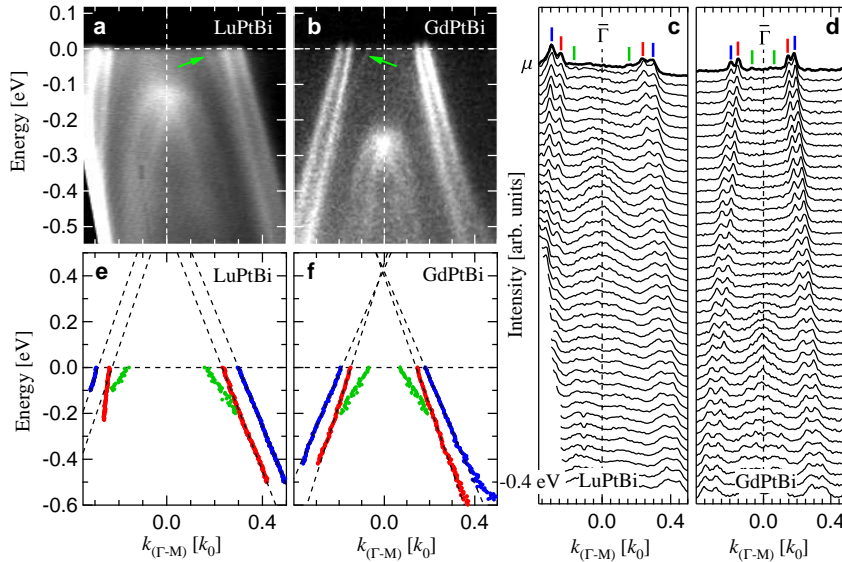

FIG. 4: Band structure analysis at the vicinity of $\bar{\Gamma}$ [red arrows in Fig. 1(e)]. Data is taken on LuPtBi and GdPtBi samples at $T = 15$ K. (a)-(b) Band dispersion maps along the $\bar{\Gamma}$-$\bar{M}$ direction. Green arrows point to the position of the inner hole band which have lower intensity than the two other hole bands. (c)-(d) Corresponding MDCs for panels (a) and (b). (e)-(f) Extraction of the band position for panels (a) and (b). By linearly extrapolating the bands above the chemical potential μ we show an approximate band crossing point (Dirac point) at $E \sim 0.4$ eV for GdPtBi.

inner one (or two, see discussion for Fig. 2). As shown in Fig. 3(h), These three (or four) bands cross μ at exactly the same k positions for all photon energies. Therefore all of them are surface bands. The data in Fig. 3 thus show, unambiguously, that a metallic surface electronic state exists in the half-Heusler compounds.

The exact number of Fermi crossings along the $\bar{\Gamma}$-$\bar{M}$ line segment is also examined in Fig. 4. The main conclusion for Fig. 4 is that there are also three (or four) visible Fermi crossings at the vicinity of $\bar{\Gamma}$ between these two Kramers' points. We show these bands on the LuPtBi and GdPtBi samples. Both on the band dispersion maps [Figs. 4(a)-(b)] and the momentum distribution curves

[MDCs, Figs. 4(c)-(d)] we see that there are two bright hole-like bands almost parallel to each other, and a much weaker inner band with lower Fermi velocity. This inner band is not easy to see in the band maps (nonetheless indicated by green arrows), but is clearly visible in the MDCs by small intensity peaks tracing down from the one marked by a green bar [also marked by a green color in Figs. 4(e)-(f)]. The same band also exists in the $\bar{\Gamma}$-$\bar{K}$ direction [Figs. 3(d)-(h)]. Same as the discussion for Figs. 2 and 3, this inner crossing is reproduced in the band calculation by two closely located spin-orbit-splitting bands that form a Kramers' pair. The brighter parallel bands form a second Kramers' pair of opposite
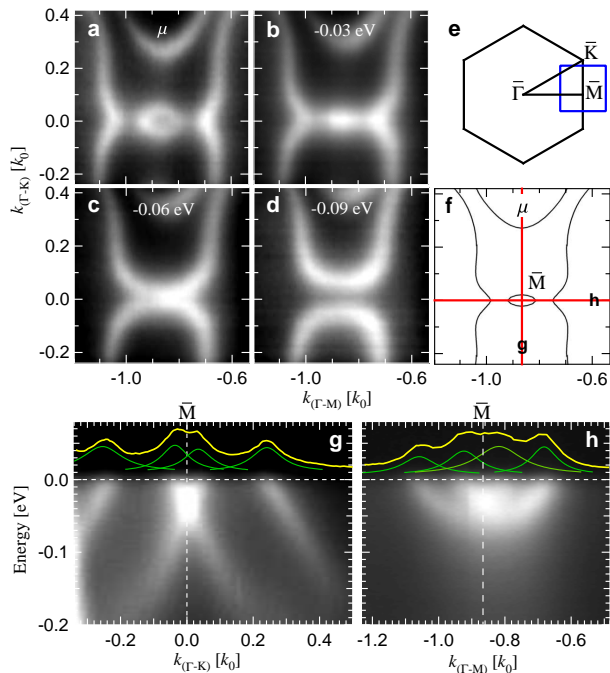
FIG. 5: Band structure analysis at the vicinity of $\bar{M}$ [red box in Fig. 1(c)]. Data is taken on LuPtBi samples. (a)-(d) Binding energy dependence of band structure near $\bar{M}$. Map location in the surface Brillouin zone is shown in Panel (e). (f) Theoretical band map at the chemical potential for GdPtBi. (g),(h) Band maps for two perpendicular directions marked by red lines in (g). There are in total two Fermi crossings along the $\bar{\Gamma}$-$\bar{M}$ line segment at the vicinity of $\bar{M}$.

total Berry phase.

In summary, we performed an ARPES survey on the electronic structure of three half-Heusler compounds RPtBi (R = Lu, Dy, Gd) which are proposed to be topological insulators. Our result show unambiguously that these materials have a metallic surface state markedly different from the calculational result on the bulk electronic structures. This surface state is reproduced with high accuracy in our band calculations. Both experiment and theory reveal several bands that cross the Fermi level. Knowledge of the exact number of these bands is possibly limited by experimental momentum resolution. Topologically non-trivial behavior is indicated with band inversion in the bulk band calculations, yet no direct consistency with such behavior is found in the ARPES results for the surface bands. For final determination of their topological classes, both an APRES measurement of ultrahigh k-resolution resolving both the bulk state and surface state contribution, and a direct calculation of the first Chern number as a topological invariant[27] are in need.

IV.   ACKNOWLEDGEMENT

spins. In Fig. 4(e)-(f) we show the linear extrapolation of the two brighter bands. In GdPtBi they are likely to reduce to a Dirac point at about 0.4 eV above μ. If the total number of crossing is four, such a configuration will give zero contribution to the total Berry phase.

In Fig. 5 we examine the bands near the $\bar{M}$ point. The k-space location of the ARPES maps [Figs. 5(a)-(d)] is shown in Fig. 5(e). Panels 5(g)-(h) present the band dispersion maps for two cuts crossing $\bar{M}$, whose positions are marked in Panel 5(f) with the band calculation result. Figs. 5(a)-(d) show that the $\bar{M}$ bands form a very special shape. At high binding energies [$E \sim -0.1$ eV, Fig. 5(d)], two U-shape bands are well separated. As binding energy decreases these two bands merge into each other and hybridize to form a central elliptical contour and two curly-bracket-like segments. The segments near each $\bar{M}$ points link together, forming another large Fermi contour enclosing the zone center $\bar{\Gamma}$. It is clear from Fig. 5(g)-(h) that there are two Fermi crossings in both the $\bar{\Gamma}$-$\bar{K}$ and $\bar{\Gamma}$-$\bar{M}$ directions. The special shape of the Fermi surface is formed by two bands that are likely to be members of another Kramers' pair. Kramers' degeneracy of spin happens at ~ 30 meV below μ. All this features are obtained with our calculation for the surface states [Fig 2(b) and 2(e)]. These two bands also give zero contribution to the

[1] M. Z. Hasan and C. L. Kane, Rev. Mod. Phys. **82**, 3045 (2010).

[2] J. E. Moore, Nature (London) **464**, 194 (2010).

[3] B. A. Bernevig, T. L. Hughes, and S.-C. Zhang, Science **314**, 1757 (2006).

[4] M. König, S. Wiedmann, C. Brüne, A. Roth, H. Buhmann, L. W. Molenkamp, X.-L. Qi, and S.-C. Zhang, Science **318**, 766 (2007).

[5] A. Roth, C. Brüne, H. Buhmann, L. W. Molenkamp, J. Maciejko, X.-L. Qi, and S.-C. Zhang, Science **325**, 294 (2009).

[6] D. Hsieh, D. Qian, L. Wray, Y. Xia, Y. S. Hor, R. J. Cava, and M. Z. Hasan, Nature (London) **452**, 970 (2008).

[7] D. Hsieh, Y. Xia, L. Wray, D. Qian, A. Pal, J. H. Dil, J. Osterwalder, F. Meier, G. Bihlmayer, C. L. Kane, Y. S. Hor, R. J. Cava, and M. Z. Hasan, Science **323**, 919 (2009).

[8] P. Roushan, J. Seo, C. V. Parker, Y. S. Hor, D. Hsieh, D. Qian, A. Richardella, M. Z. Hasan, R. J. Cava, and A. Yazdani, Nature (London) **460**, 1106 (2009).

[9] H. Zhang, C.-X. Liu, X.-L. Qi, X. Dai, Z. Fang, S.-C. Zhang, Nature Physics **5**, 438 (2009).

[10] Y. L. Chen, J. G. Analytis, J.-H. Chu, Z. K. Liu, S.-K. Mo, X. L. Qi, H. J. Zhang, D. H. Lu, X. Dai, Z. Fang, S. C. Zhang, I. R. Fisher, Z. Hussain, and Z.-X. Shen, Science **325**, 178 (2009).

[11] S. Chadov, X.-L. Qi, J. Kübler, G. H. Fecher, C. Felser, and S.-C. Zhang, Nature Materials **9**, 541 (2010).

[12] H. Lin, L. A. Wray, Y. Xia, S. Xu, S. Jia, R. J. Cava, A. Bansil, and M. Z. Hasan, Nature Materials **9**, 546 (2010).

[13] P. C. Canfield, J. D. Thompson, W. P. Beyermann, A. Lacerda, M. F. Hundley, E. Peterson, Z. Fisk, and H. R. Ott, J. Appl. Phys. **70**, 5800 (1991).

[14] G. Goll, M. Marz, A. Hamann, T. Tomanic, K. Grube, T. Yoshino, and T. Takabatake Physica B **403**, 1065 (2008).

[15] Z. Fisk, P. C. Canfield, W. P. Beyermann, J. D. Thompson, M. F. Hundley, H. R. Ott, E. Felder, M. B. Maple, M. A. Lopez de la Torre, P. Visani, and C. L. Seaman, Phys. Rev. Lett. **67**, 3310 (1991).

[16] D. Hsieh, Y. Xia, D. Qian, L. Wray, J. H. Dil, F. Meier, J. Osterwalder, L. Patthey, J. G. Checkelsky, N. P. Ong, A. V. Fedorov, H. Lin, A. Bansil, D. Grauer, Y. S. Hor, R. J. Cava and M. Z. Hasan, Nature (London) **460**, 1101 (2009).

[17] C. L. Kane and E. J. Mele, Phys. Rev. Lett. **95**, 146802 (2005).

[18] P. C. Canfield and Z. Fisk, Philos. Mag. B **65**, 1117 (1992).

[19] P. Blaha, K. Schwarz, G. K. H. Madsen, D. Kvasnick and J. Luitz, WIEN2k, An augmented plane wave plus local orbitals program for calculation crystal properties (K. Schwarz, TU wien, Austria, 2001) ISBN 3-9501031-1-2.

[20] J. P. Perdew and Y. Wang, Phys. Rev. B **45**, 13244 (1992).

[21] M. G. Haase, T. Schmit, C. G. Richter, H. Block, and W. Jeitschko, J. Solid State Chem. **168**, 18 (2002).

[22] V. N. Antonov, P. M. Oppeneer, A. N. Yaresko, A. Y. Perlov, and T. Kraft, Phys. Rev. B **56**, 13012 (1997).

[23] W. Al-Sawai, Hsin Lin, R. S. Markiewicz, L. A. Wray, Y. Xia, S.-Y. Xu, M. Z. Hasan, and A. Bansil, Phys. Rev. B **82**, 125208 (2010).

[24] L. Fu, Phys. Rev. Lett. **103**, 266801 (2009).

[25] Di Xiao, Yugui Yao, Wanxiang Feng, Jun Wen, Wenguang Zhu, Xing-Qiu Chen, G. Malcolm Stocks and Zhenyu Zhang, Phys. Rev. Lett. **105**, 096404 (2010).

[26] K. Park, J. J. Heremans, V. W. Scarola, and D. Minic, arXiv:1005.3476 (unpublished) (2010).

[27] X.-L. Qi, T. L. Hughes, and S.-C. Zhang, Phys. Rev. B **78**, 195424 (2008) and references therein.